Annals of Botany **120**: 577–590, 2017
doi:10.1093/aob/mcx091, available online at www.academic.oup.com/aob

ANNALS OF BOTANY
Founded 1887

A role for LAX2 in regulating xylem development and lateral-vein symmetry in the leaf

Guillermo S. Moreno-Piovano[1,†], Javier E. Moreno[1,†], Julieta V. Cabello[1], Agustín L. Arce[1], María E. Otegui[2] and Raquel L. Chan[1,*]

[1]*Instituto de Agrobiotecnología del Litoral, Universidad Nacional del Litoral - CONICET, Facultad de Bioquímica y Ciencias Biológicas, Colectora Ruta Nacional 168 km 0, Santa Fe, Argentina and* [2]*Facultad de Agronomía, Universidad de Buenos Aires, CONICET, Argentina*
**For correspondence. E-mail rchan@fbcb.unl.edu.ar*
[†]G.S.M.P. and J.E.M. contributed equally to this work.

Received: 5 October 2016 Returned for revision: 23 February 2017 Editorial decision: 14 May 2017 Accepted: 9 June 2017

• **Background and Aims** The symmetry of venation patterning in leaves is highly conserved within a plant species. Auxins are involved in this process and also in xylem vasculature development. Studying transgenic Arabidopsis plants ectopically expressing the sunflower transcription factor HaHB4, it was observed that there was a significant lateral-vein asymmetry in leaves and in xylem formation compared to wild type plants. To unravel the molecular mechanisms behind this phenotype, genes differentially expressed in these plants and related to auxin influx were investigated.
• **Methods** Candidate genes responsible for the observed phenotypes were selected using a co-expression analysis. Single and multiple mutants in auxin influx carriers were characterized by morphological, physiological and molecular techniques. The analysis was further complemented by restoring the wild type (WT) phenotype by mutant complementation studies and using transgenic soybean plants ectopically expressing *HaHB4*.
• **Key Results** *LAX2*, down-regulated in *HaHB4* transgenic plants, was bioinformatically chosen as a candidate gene. The quadruple mutant *aux1 lax1 lax2 lax3* and the single mutants, except lax1, presented an enhanced asymmetry in venation patterning. Additionally, the xylem vasculature of the *lax2* mutant and the *HaHB4*-expressing plants differed from the WT vasculature, including increased xylem length and number of xylem cell rows. Complementation of the *lax2* mutant with the *LAX2* gene restored both lateral-vein symmetry and xylem/stem area ratio in the stem, showing that auxin homeostasis is required to achieve normal vascular development. Interestingly, soybean plants ectopically expressing *HaHB4* also showed an increased asymmetry in the venation patterning, accompanied by the repression of several *GmLAX* genes.
• **Conclusions** Auxin influx carriers have a significant role in leaf venation pattering in leaves and, in particular, *LAX2* is required for normal xylem development, probablt controlling auxin homeostasis.

Key words: Auxin influx carriers; HD-Zip I; *HaHB4*; *LAX2*; venation symmetry; vascular patterning; xylem organization.

INTRODUCTION

Organisms have evolved complex traits to cope with the surrounding environment. Biological systems show high resilience to external perturbations that are somehow buffered by the regulatory interaction of developmental networks (Masel and Siegal, 2009; Lempe *et al*., 2013; Payne and Wagner, 2015). In certain scenarios, restoration of the individual's homeostasis cannot be fully reached, leaving a permanent mark on developmental patterning (Leamy and Klingenberg, 2005). Ecologists have largely recorded this environmental footprint in the development of organ symmetry, such as symmetry of wings and embryos in *Drosophila* (Klingenberg *et al*., 1998; Houchmandzadeh *et al*., 2002), mandibles in mice (Leamy *et al*., 2002), and leaf-lamina (Muñoz-Nortes *et al*., 2014; Graham *et al*., 2015) and leaf-venation patterning (Aloni *et al*., 2003) in plants. Developmental gene regulatory networks play a central role in the resilience to environmental stress. For example, the heat-shock protein 90 (Hsp90) chaperone appears to be a conserved molecular capacitor in phylogenetically distant groups (Rutherford and Lindquist, 1998; Queitsch *et al*., 2002). These results underlined the role of Hsp90 in buffering the genetic variation within a population, and also highlighted the fact that genetic variation can be exposed when buffering systems are strained by the environment. Plant ecologists have scored the impact of environmental stress on organs with bilateral symmetry, traditionally on leaves with a central vein. Recently, it was reported that slight differences in leaf bilateral symmetry of Arabidopsis and tomato plants was correlated to a differential auxin distribution on phyllotactic patterning (Chitwood *et al*., 2012). Plant symmetry has also been studied on venation patterning (Aloni, 2010). In this regard, it has been proposed that auxin distribution in the leaf lamina is involved in the control of venation symmetry (Aloni, 2001; Aloni *et al*., 2003). These studies combined experiments with exogenous application of auxin and the use of the synthetic auxin-responsive

promoter DR5. This promoter fused to the *GUS*-reporter gene revealed strong β-glucuronidase (GUS) activity on hydathodes of developing leaves. The high auxin accumulation at the still differentiating hydathodes may regulate the differentiation of upper secondary veins, thus controlling venation symmetry (Aloni *et al*., 2003). This model was supported by the following observations: (1) mutants with altered patterns of auxin accumulation translated into changes of the normal venation patterning (Koizumi *et al*., 2000; Aloni *et al*., 2003), and (2) exogenous application of auxin-transport inhibitors or synthetic auxin analogues to Arabidopsis leaves caused an altered number of secondary veins (Mattsson *et al*., 1999; Sieburth, 1999; Aloni, 2010).

Auxins are exported and imported from cell to cell using efflux and influx carriers: PIN and AUX/LAX, respectively. Auxin homeostasis in the leaf lamina is critical to achieve the appropriate growth response, and auxin transport appears to be critical for auxin homeostasis along the whole plant body. Auxin homeostasis includes auxin distribution, hormone synthesis and inactivation rates, and stability of receptors and repressors (Petrasek and Friml, 2009; Vanneste and Friml, 2009; Salehin *et al*., 2015). It is interesting to note that members of both the *PIN* and the *AUX/LAX* gene families have evolved sub-functionalization. For instance, the *aux1* mutant produced inhibition of root hair elongation and altered gravitropic response (R. Swarup *et al*., 2005, 2007), *lax1* and *lax3* mutants produced a decrease in lateral root formation (K. Swarup *et al*., 2008), and the *lax2* mutant caused vascular breaks in cotyledons (Peret *et al*., 2012). In addition, leaf phyllotaxy was significantly altered by mutations in *AUX1* and *LAX1* genes (Bainbridge *et al*., 2008). Recently, a direct connection between auxin influx carriers and vasculature development has been shown in Arabidopsis. The quadruple *aux1 lax1 lax2 lax3* (hereafter *quad*) mutant, but not the single *aux*/*lax* mutants, developed fewer and less-dense vascular bundles than the wild type (WT) only when grown under short-day conditions (Fabregas *et al*., 2015). Yet, the vascular bundle organization of the *quad* mutant was uneven, with an increased number of procambial and xylem cells (the latter of enhanced size) both in shoots and in roots (Fabregas *et al*., 2015).

Transcription factors (TFs) are modular proteins able to articulate the perception of environmental signals to cellular responses. The homeodomain-leucine zipper (HD-Zip) TF family coordinates different aspects of the plant biology including, but not limited to, plant biotic and abiotic stress tolerance, leaf shape and polarity, vascular development, and root and trichome formation (Capella *et al*., 2015*b*). The HD-Zip family comprises four subfamilies, I–IV. HD-Zip subfamily I (hereafter HD-Zip I) TFs were initially associated with plant responses to the environment and more recently these regulatory proteins have been found to participate in developmental processes (Perotti *et al*., 2017).

HaHB4 is an HD-Zip I TF from *Helianthus annuus*, defined by phylogenetic analysis as an uncommon member given its extremely short and divergent carboxy-terminus (Arce *et al*., 2011). *HaHB4* ectopic expression improved drought and salinity tolerance in transgenic Arabidopsis and soybean plants with no penalty on yield under control conditions (Dezar *et al*., 2005; Arcadia-Biosciences, 2015). In Arabidopsis, this increased tolerance is indeed part of a complex phenotype that includes delayed senescence and enhanced resistance to herbivory (Manavella *et al*., 2006, 2008). However, the complex phenotype triggered by *HaHB4* in transgenic plants is not well understood.

In the current study, Arabidopsis and soybean transgenic plants expressing *HaHB4* were used as a prospecting tool to uncover novel traits related to signal transduction pathways regulated by this TF. A co-expression analysis performed on genes differentially expressed in Arabidopsis *HaHB4*-transgenic plants allowed us to identify *LAX2* as a potential down-regulated target of HaHB4. Then, the phenotypes of single and multiple mutant alleles of the *AUX*/*LAX* gene family were characterized. An increased asymmetry in the venation patterning of Arabidopsis *lax2* mutant alleles was observed. We also revealed the functional role of the auxin influx carrier *LAX2* as a negative regulator of xylem development in Arabidopsis plants. The asymmetric venation phenotype was also observed in *35S:HaHB4* Arabidopsis leaves as well as in soybean plants expressing *HaHB4* under the control of its native promoter. Finally, we linked this venation phenotype to the LAX2 auxin influx carrier based on *HaHB4*-mediated down-regulation of *LAX2* expression in Arabidopsis and *GmLAX* genes in soybean.

MATERIALS AND METHODS

Plant material, growth conditions and treatments

Arabidopsis thaliana plants were grown on Klasmann Substrat No. 1 compost (Klasmann-Deilmann GmbH, Geeste, Germany) in a growth chamber at 22–24 °C under long-day conditions (16/8-h light/dark cycles) with a light intensity of 120 μmol m^{-2} s^{-1} in 8 × 7-cm pots. In all Arabidopsis experiments the Col-0 ecotype was used as the WT control and four plants were planted per pot.

A total of six Arabidopsis mutant genotypes were grown; the mutants used were the *lax2-1*, *lax2-2*, *lax1*, *lax3*, *aux1-21* and *quad*, all in the Col-0 background. *Arabidopsis* null mutant lines *lax2-1* (dSpm line) and *lax2-2* (GK_345D11) were described previously (Peret *et al*., 2012). Arabidopsis plants bearing the *HaHB4* cDNA driven by the 35S cauliflower mosaic virus promoter were also previously described (Dezar *et al*., 2005).

In the case of soybean (*Glycine max* 'Williams 82'), two genotypes were evaluated. Seeds of the WT and those expressing the sunflower *HaHB4* cDNA under its native promoter (named here as *b10H* event) were obtained from INDEAR (Rosario, Argentina). Soybean plants of each genotype were grown in 20-litre pots (five plants per pot) up to the V7 developmental stage. Pots bearing transgenic or control plants were arranged in a glasshouse under long-day conditions (approx. 15/9-h light/dark cycles), with daily temperatures fluctuating between 19 °C (during the night) and 40 °C (during the day). Although the temperature amplitude reached almost 30 °C in a day, all plant genotypes were grown together and exposed to the same conditions.

Two water regimes (irrigated and water deficit) were imposed between developmental stages V5 and V7, representing 14 d of treatment in December–January at our latitude. During this period, one group of plants (20 plants of each genotype) received adequate water supply whereas irrigation was arrested in

the second group (20 plants). Plant measurements were taken at the V7 stage in both groups.

RNA isolation and expression analyses by real time RT-PCR

Total RNA for real-time RT-PCR was isolated from Arabidopsis leaves or stems using Trizol reagent (Invitrogen, Carlsbad, CA, USA) according to the manufacturer's instructions. Total RNA (1 μg) was reverse-transcribed using oligo(dT)18 and M-MLV reverse transcriptase II (Promega, Fitchburg, WI, USA).

Total RNA from soybean was isolated from the terminal foliole of the last fully developed leaf of three individual soybean plants (V7 stage). The samples were processed using the same reagents and protocol described for Arabidopsis tissue.

Quantitative real-time PCR (RT-qPCR) was performed using a Mx3000P Multiplex qPCR system (Stratagene, La Jolla, CA, USA) as described by Capella *et al*. (2015*a*) and using the primers listed in Supplementary Data Table S1. Transcript levels were normalized by applying the ΔΔCt method. Actin transcripts (*ACTIN2* and *ACTIN8* for Arabidopsis and *GmActin* for soybean) were used as internal standards to normalize differences in template amounts. Three biological replicates, obtained by pooling tissue from three to four individual plants and tested in duplicate, were used to calculate the standard deviation.

Genetic constructs and Arabidopsis plant transformation

A Gateway-compatible plasmid containing the LAX2 cDNA was obtained from ABRC (Ohio State University, Columbus; clone U15627) and recombined into the pJV126 expression vector (gift of Dr D. Weigel, Max Planck Institute, Tübingen-Germany) using the Gateway LR Clonase II Enzyme Mix (Thermo Fisher, Waltham, MA, USA) according to the manufacturer's instructions. The pJV126 vector is derived from the pGreen vector series: genetic fragments were recombined by Gateway (Life Technologies) cloning into a modified pGreen vector (pFK210) conferring resistance to BASTA (Hellens *et al*., 2000). A *35S CaMV* promoter drives the expression of an N-terminal fusion protein with mCitrine, here named *35S:mCitrine:LAX2*. A sequence-verified clone was used for transforming *Agrobacterium tumefaciens* strain LBA4404 and then generating transgenic Arabidopsis plants using the floral dip method (Clough and Bent, 1998). To screen for high-expressing lines, we followed a two-step selection process. First, T1 plants were grown in soil for 7 d and watered with a solution containing 0·3 μM glufosinate (Liberty; Bayer CropScience, Leverkusen, Germany), and second, we used a Leica TCS SP8 Compact confocal microscope to screen for highly fluorescent seedlings that accumulated mCitrine-LAX2 fusion protein. T2 plants containing a single transfer DNA insertion (as determined by 3 : 1 segregation of herbicide resistance) were further used in experiments. All experiments were done with at least three independent transgenic lines probably containing a single T-DNA. Multiple tandem insertions cannot be ruled out with this selection procedure and therefore several independent lines were evaluated simultaneously. Homozygous T3 lines were further used to analyse transgene expression levels and plant phenotypes.

Microarray data analysis and clustering

The transcriptome analysis of *35S:HaHB4* Arabidopsis plants was previously reported (Manavella *et al*., 2006). These data were used in an exploratory analysis in which genes responding to *HaHB4* overexpression but not to drought stress in WT or in *35S:HaHB4* plants were selected. More precisely, the chosen set of genes satisfied the following condition: an absolute $\log_2$ expression ratio greater than 0·5 in *35S:HaHB4* vs. WT plants, and lower than 0·5 in stressed vs. non-stressed plants. This resulted in a list of 497 genes, which was further used in a co-expression analysis with public expression datasets using the R environment for statistical computing (https://www.r-project.org/). This analysis consisted in first retrieving public Arabidopsis microarray experiments from the AtGenExpress project (http://jsp.weigelworld.org/AtGenExpress/resources/). The gene expression datasets considered were: abiotic stress in roots, shoots and cell cultures (Kilian *et al*., 2007), pathogen treatment and the developmental series (Schmid *et al*., 2005). Expression profiles of the 446 genes with measurements in the microarrays, i.e. presenting probesets in the Affymetrix ATH1 microarray, were then pairwise correlated. Correlations were converted to distances by subtracting their absolute value from 1, and the resulting matrix was used to perform a hierarchical clustering with the average agglomeration method. Gene clusters were then defined by cutting the tree at 0·4, and their genes were analysed using the GeneMANIA server (Warde-Farley *et al*., 2010). Description of the cluster is given in Supplementary Data Table S2.

Histology and microscopy

Arabidopsis inflorescence stem sections were harvested from the base of the first internode of 30-cm-high stems. Soybean stem sections were collected from the base of the epicotyl of V7 plants. In all cases, sections 0·5–1 cm in length were fixed at 24 °C for 1 h in a solution containing 3·7 % formaldehyde, 5 % acetic acid and 47·5 % ethanol, and then dehydrated through a graded series of ethanol solutions (70, 80, 90, 96 and 100 %; 30 min each) followed by 1 h in 100 % xylene. The samples were placed into plastic moulds and finally embedded with 100 % Histoplast (Biopack, Argentina). Each block was incubated overnight at room temperature to ensure solidification. Transverse stem sections (10 μm thick) were obtained using a Leica Microtome (RM2125; Leica, Wetzlar, Germany). Cross sections were mounted on slides coated with 50 mg mL^{-1} poly-D-lysine (Sigma Chemical Co., St. Louis, MO, USA) in 10 mM Tris-HCl, pH 8·0, and dried for 16 h at 37 °C. After removing the paraffin with 100 % xylene for 15 min at room temperature, sections were rehydrated using a graded series of ethanol (100, 96, 90, 80, 70 and 50 %; 1 min each) to finish in distilled water. Samples were then stained with 0·1 % Toluidine blue, rinsed, and mounted on Canadian balsam (Biopack) for microscopic visualization in an Eclipse E200 Microscope (Nikon, Tokyo, Japan) equipped with a Nikon Coolpix L810 camera. Toluidine blue was used to

differentially stain primary and secondary cell walls. Primary cell walls are pink and secondary cell walls stain blue or blue-green. In this way, it is possible to distinguish between phloem and xylem cells since cells found in phloem have primary cell walls (cellulose) whereas xylem cells have both primary and secondary cell walls rich in lignin. Forty vascular bundles of eight cross-sections were evaluated for each genotype and treatment (40 vascular bundles per genotype/treatment). Quantification of vascular bundle (VB) parameters (xylem ratio, number of cells and VB length) was performed using ImageJ software (Schneider *et al*., 2012) as follows: both xylem length and number of xylem cell rows were measured on a straight line traced from the last procambium cell layer to the inner xylem cells facing the centre of the stem. The xylem/stem area ratio is the proportion that the xylem represents on the total stem area (xylem area/total stem area).

Venation patterning in leaves of adult plants

The study of venation patterning was performed on a fully developed leaf of a 30-d-old plant. Based on previous morphological studies on Arabidopsis plants (Boyes *et al*., 2001; Farmer *et al*., 2013), we chose the rosette true leaf No. 5. Leaf No. 5, considering only true leaves (Farmer *et al*., 2013), of Arabidopsis plants was harvested and cleared overnight in 70 % ethanol. Leaves were imaged using a Leica MZ10F stereomicroscope coupled to a DFC7000 T camera (Leica). In most cases, pictures of the general leaf aspect were obtained by merging two photographs (Leica merge tool), the upper and lower half of the leaf. In some cases, when the software failed to merge them, the two leaf pictures were manually overlaid. Venation patterning was recorded in leaf No. 5 using two complementary traits: (1) secondary vein-attachment-site distance and (2) lateral-vein asymmetry index. Vein-attachment-site distance was scored as the distance between the attachment points of the two secondary veins of the third pair on the midvein using ImageJ software. In addition, Arabidopsis lateral-vein asymmetry index was scored as the fraction between the number of vein pairs asymmetrically distributed on the midvein divided by the total number of vein-pairs in the leaf. In the case of soybean leaves, venation patterning was recorded counting the fraction of vein pairs asymmetrically developed (asymmetric vein pairs/total vein pairs) on the midvein of the terminal foliole of the last fully developed leaf. In all cases, a total of six plants of each genotype were scored.

Plant phenotyping

Different plant architecture parameters were scored on 35-d-old Arabidopsis plants. Age of plants was counted as days after sowing. Measurements were performed at least on 12 plants per treatment. Evaluated traits were inflorescence stem height (with a ruler), main stem width (with a Vernier caliper), number of secondary branches, number of secondary stems, total silique number and yield.

Leaf conductance was measured at the V7 stage in the terminal foliole of the last fully developed leaf of soybean plants, excluding the mid-rib area. Measurements were performed near midday by means of an SC-1 Leaf Porometer (Decagon Devices Inc., Pullman, WA, USA), on both leaf sides (adaxial and abaxial) and using an integration time of 30 s. Three pots for each combination of genotype (W82 and b10H plants) and soil water condition (irrigated or water-stressed) were analysed. In each pot, representing an individual replica, the average of three plants was considered as a value. Standard deviation was calculated taking the values of three pots.

Statistical analysis

Venation, xylem patterning and xylem/stem ratio were analysed using a one way ANOVA with genotype as the main factor. Significant ($P < 0{\cdot}05$) differences between means were analysed using *post-hoc* Tukey comparisons. In soybean plants growing under irrigated or water deficit conditions, data were analysed using a two-way ANOVA with water regime and genotype as factors. When interaction terms were significant ($P < 0{\cdot}05$), differences between means were analysed using Tukey comparisons. When needed, appropriate transformations of the primary data were used to meet the assumptions of the analysis. In all cases, differences between means are indicated by different letters.

RESULTS

Ectopic expression of HaHB4 *in Arabidopsis leaves induces similar changes in venation patterning to those observed in auxin influx carrier mutants*

The expression of the sunflower HD-Zip I-encoding gene *HaHB4* under the *35S CaMV* promoter generated a wide transcriptional rearrangement affecting different plant traits such as drought tolerance, ethylene sensitivity and jasmonate-induced defences (Dezar *et al*., 2005; Manavella *et al*., 2006, 2008). To further understand the molecular physiology behind this complex phenotype, we performed a new analysis on the previously reported microarray results of Arabidopsis *35S:HaHB4* plants (Manavella *et al*., 2006), which involved two-colour microarrays with the following transcriptome comparisons: WT plants in control vs. drought conditions, WT vs. *35:HaHB4* plants in control conditions, and *35:HaHB4* plants in drought vs. control conditions. Briefly, the procedure consisted in selecting a set of genes responding to *HaHB4* overexpression but not to drought stress in WT or in *35S:HaHB4* plants, and then using them in a co-expression study with publicly available expression datasets. This allowed us to identify gene co-expression clusters that, after functional enrichment analysis, could potentially help us in dissecting the physiological role of *HaHB4* in transgenic plants. This approach identified a gene cluster including the *LAX2* (*like-AUXIN RESISTANT 2*) gene and other auxin-related genes, such as *TAR2* and *AIR9* (Fig. 1A). *AUX*/*LAX* transcript levels were evaluated by RT-qPCR in *lax2-1*, *lax2-2* mutants and *35S:HaHB4* plants resulting in significantly different patterns (Fig. 1B). Whereas *AUX1* and *LAX1* expression was similar between genotypes, *LAX3* expression was significantly upregulated in *35S:HaHB4* (OE) plants. On the other side, *LAX2* was the only *AUX*/*LAX* gene family member showing a strong repression by *HaHB4* (Fig. 1B), validating expression values observed in the microarray ($\log_2$ fold change $= 0{\cdot}58 \pm 0{\cdot}17$). This result led us to explore the relationship among *AUX*/*LAX*

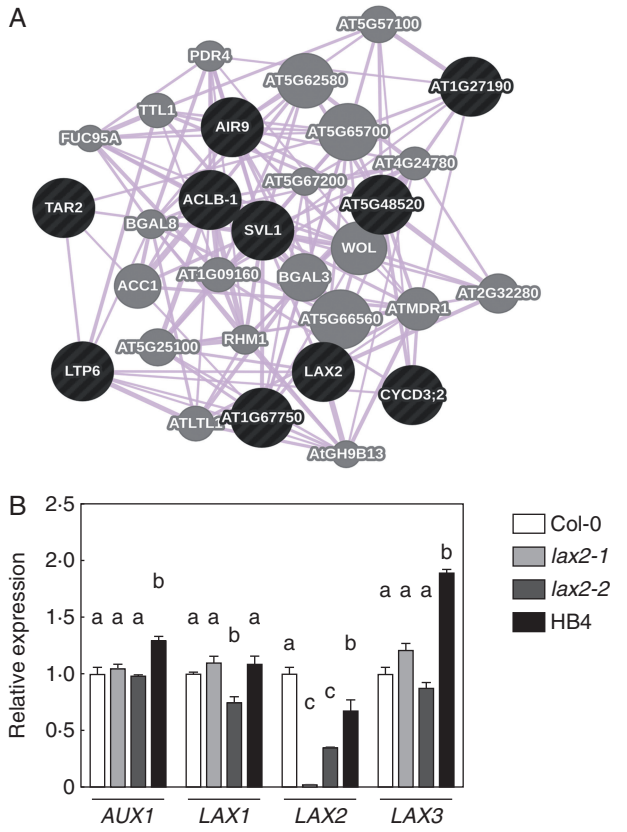

FIG. 1. *HaHB4* represses the expression of *LAX2* in Arabidopsis transgenic plants. (A) Co-expression of genes in the cluster generated using the GeneMania software package. The cluster is statistically enriched in genes related to auxin homeostasis, i.e. *LAX2*, *TAR2* and *AIR9* ($P \leq 0{\cdot}05$). Black nodes represent the list of query genes used in GeneMania. Grey nodes represent genes that were associated by a co-expression pattern according to GeneMania. (B) Relative transcript levels of *AUX/LAX* family members in rosette leaves of 20-d-old plants of WT (Col-0), *lax2-1*, *lax2-2* and *HaHB4* (displayed here as HB4) plants. *AUX/LAX* transcript abundance was measured and expressed relative to the level detected in Col-0 plants. Different letters indicate significant differences between means ($P < 0{\cdot}05$, Tukey test).

genes, in particular between *LAX2* and the *HaHB4*-induced phenotypes.

It is well known that plant water transport depends on both xylem organization and vein architecture (for a review, see Prado and Maurel, 2013). Given that *35S:HaHB4* plants have enhanced drought tolerance and that auxin modulates venation patterning in leaves and vascular development, these auxin-related characteristics were further investigated in *AUX/LAX* gene mutants and in *35S:HaHB4* plants. To evaluate the leaf venation patterning, we defined two robust parameters. First, we scored the distance between the attachment points of the lateral veins of the third pair on the midvein (Fig. 2A). Second, we recorded the lateral-vein asymmetry index as a ratio between the number of asymmetric lateral vein pairs divided by the total number of lateral vein pairs in the leaf lamina (Fig. 2A). All these parameters were scored on leaf numbers 5 and 6 of 30-d-old Arabidopsis plants because at this stage the leaf laminae were fully expanded (Boyes *et al*., 2001). For simplicity, we show here only data for leaf number 5. Lateral-vein asymmetry index was also recorded on leaf number 5 at younger stages. At these earlier stages, we were not able to detect significant differences on leaf asymmetry, probably because leaf expansion was not complete, and therefore lateral-vein attachment sites were still too close to detect the differences. It is noteworthy to mention that although vein patterning seems to be a robust developmental response, all the analysed plant genotypes had a certain level of variation, even leaves of WT plants (Fig. 2C, D). We found that *35S:HaHB4* leaves had greater asymmetry in the venation pattern compared to the vein-attachment sites of WT leaves (Fig. 2B). In this regard, the distance between the attachment sites of the third vein pair and the lateral-vein asymmetry index of *35S:HaHB4* leaves were significantly higher than in the WT (Fig. 2C, D).

Since *LAX2* is repressed in *35S:HaHB4* transgenic plants, we wondered whether auxin influx carriers belonging to the *AUX/LAX* gene family may contribute to the modulation of the venation patterning in leaves. As observed for *35S:HaHB4* leaves, the venation patterning of all single mutants (*aux1-21*, *lax2-1* and *lax2-2* and *lax3*) but *lax1* and the *quad* mutant showed an increased asymmetry compared to WT leaves (Fig. 2B–D). The increased asymmetry in venation patterning of *lax* mutants was the result of a higher distance between the attachment sites of the third vein-pair (Fig. 2C) and a higher lateral-vein asymmetry index (Fig. 2D). Based on these results, we showed that the ectopic expression of *HaHB4* as well as *aux*/*lax* mutations promoted changes in venation asymmetry in Arabidopsis leaves.

HaHB4 *and* LAX2 *control xylem development in the inflorescence stem of Arabidopsis*

Given that *HaHB4* repressed the expression of only one *AUX/LAX* gene – *LAX2* – and *lax2* mutant alleles displayed a similar phenotype to *35S:HaHB4* plants, we decided to further explore the role of *LAX2* in vascular development. For this, a detailed phenotypic comparison of *lax2* mutant alleles (*lax2-1* and *lax2-2*) and *35S:HaHB4* plants was carried out. The most relevant resemblance between these genotypes was related to the inflorescence stem width, which was significantly wider in the three genotypes with respect to WT plants (Fig. 3A). However, other stem traits showed a significant change in *35S:HaHB4* plants but remained constant in plants of the WT and *lax2* genotypes (Fig. 3B and Fig. S1).

To further examine stem-related traits, basal stem cross-sections of the inflorescence stem were prepared, and different VB attributes were evaluated, including area, length and number of cell rows (Fig. 4B). Both the total xylem length and the number of xylem cell rows were significantly higher in *lax2* mutants and *35S:HaHB4* plants (Fig. 4A–D). In agreement with a previous report, *aux1*, *lax1*, *lax3* and *quad* mutant plants growing under long day conditions did not differ in VB organization (Fabregas *et al*., 2015). Furthermore, we recorded the xylem/stem area ratio calculated as the fraction of total xylem area with respect to the total stem area ratio. This parameter reflects the proportion of xylem in the total stem area. Again, no difference was detected for this trait among the *aux1*, *lax1* and *lax3* single mutants (Fig. 4E), whereas a slight but significant decrease was computed for the *quad* mutant as compared to the WT (Fig. 4). Notably, we observed a significant increase in the proportion of the mentioned ratio among the *lax2* mutant and *35S:HaHB4* plants as compared to stem cross-sections of the

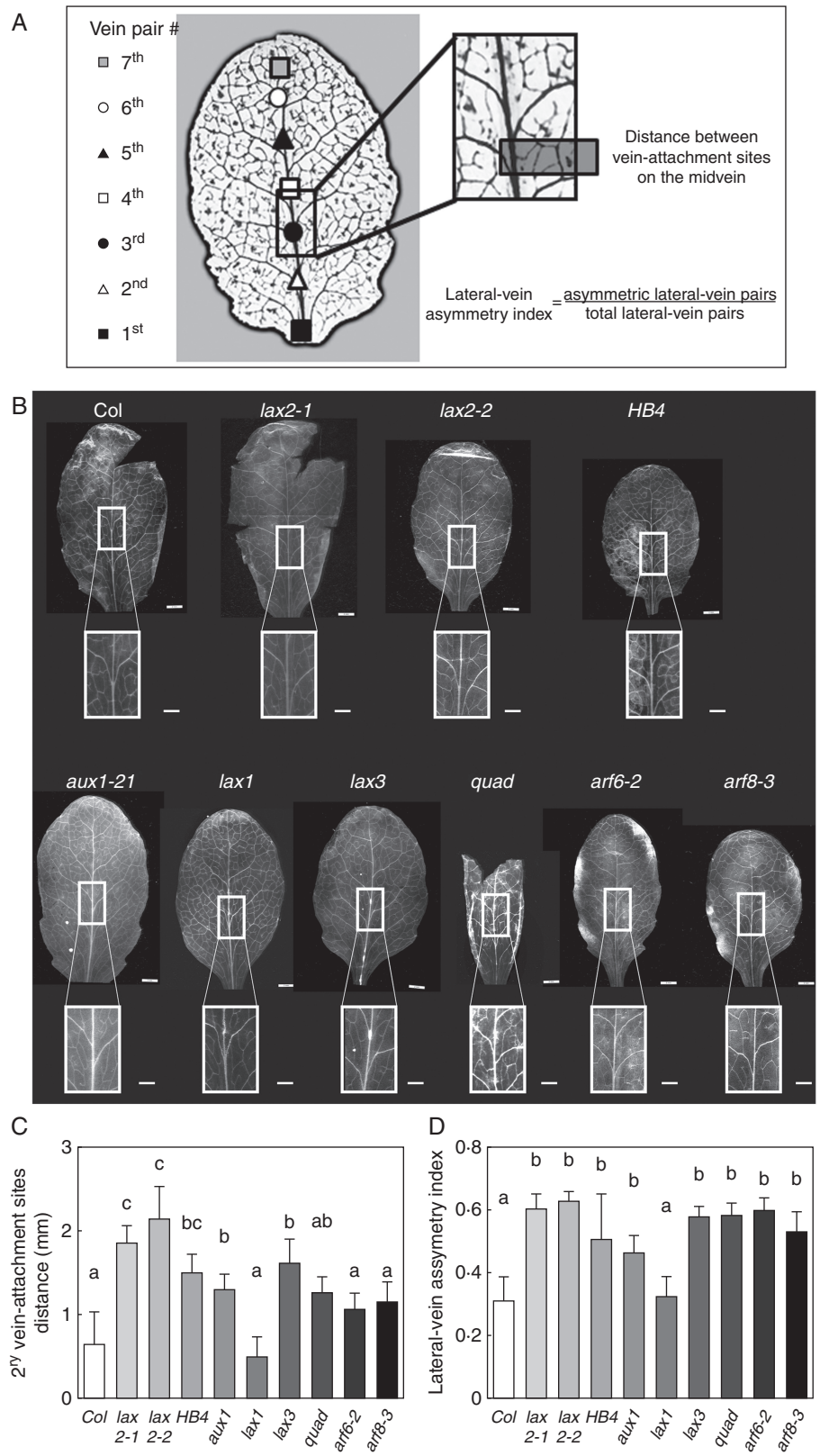

FIG. 2. Both *lax2* mutants and *35:HaHB4* leaves have enhanced asymmetry on lateral-vein attachment site of the midvein resulting in leaves with increased asymmetry in venation patterning. (A) Leaf diagram showing the parameters measured on the 5th leaf lamina. (B) Illustrative photographs of leaf number 5 and the corresponding inset showing a zoom on the third vein pair of Col-0, *lax2-1*, *lax2-2*, *35S:HaHB4*, *aux1-21*, *lax1*, *lax3*, *quad*, *arf6-2* and *arf8-3* genotypes. Whole-leaf scale bar represents 0·5 cm, whereas leaf-inset scale bar represents 1·0 mm. (C) Average distance between the two attachment sites of the lateral veins of the third pair. (D) Lateral-vein asymmetry index calculated as described in Methods. Thin bars represent s.e. Different small letters indicate significant differences ($P < 0{\cdot}05$, Tukey test).

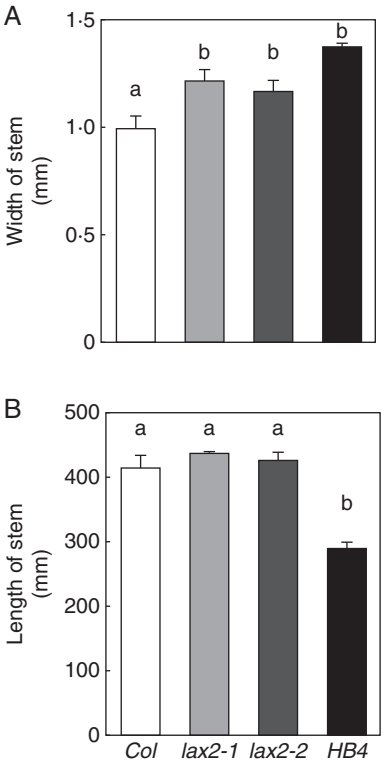

FIG. 3. Both *lax2* mutants and *35:HaHB4* plants exhibit a wider inflorescence stem than WT plants. Genotype effects on both main stem height (A) and width (B) of WT, *lax2-1* and *lax2-2* mutant alleles, and *35:HaHB4* plants. Thin bars represent s.e. Different letters indicate significant differences ($P < 0{\cdot}05$, Tukey test).

WT (Fig. 4E). This change was mostly explained by an increased number of xylem cell rows that caused an increased total xylem length (Fig. 4C, D).

Enhanced xylem development in the lax2 *mutant is not explained by apparent changes in the expression patterns of HD-Zip III and KANADI TFs*

Phloem and xylem development relies on a complex regulation between HD-Zip III and KANADI TFs, with a central role for the phytohormone auxin in activating cell differentiation (Huang *et al*., 2014; Ilegems *et al*., 2010). We wondered if this increase in xylem development might be the consequence of the missexpression of HD-Zip III and KANADI TFs in the inflorescence stem. To answer this question, we quantified the expression of several HD-Zip III and KANADI genes in the last 3 cm of the inflorescence stem, where vascular-bundle differentiation is still an on-going process (Ilegems *et al*., 2010; Lucas *et al*., 2013). RT-qPCR showed no differential expression for these genes, either in *lax2-1* or in *lax2-2* mutants (Fig. 5). On the other hand, *HaHB4* up-regulated the expression of most *HD-Zip III* and *KANADI* genes in the same tissue samples (Fig. 5).

Complementation assays with LAX2 *restores the xylem ratio in the* lax2-2 *mutant*

A transgenic complementation assay of the *lax2-2* mutant was conducted to test the functional role of *LAX2* in changing the xylem ratio in inflorescence stems, probably as a consequence of alterations in auxin transport (Peret *et al*., 2012). In parallel with the *lax2-2* mutant, we transformed plants of the Col-0 background as a control. In each case, we obtained 20 independent transgenic lines. Eleven independent transgenic lines of each genetic background were screened using a confocal microscope. From high-expressing lines, only those segregating as harbouring T-DNA insertion were kept for later studies. Within this group, we used RT-qPCR to screen T2 plants for lines presenting high levels of the mRNA encoding for the fusion protein mCitrine-LAX2 (Supplementary Data Fig. S2A). We selected two lines, A and B, for further characterization. Additionally, we checked the expression pattern of the other *AUX/LAX* family members. These lines showed a significant decrease in the expression of the other *AUX/LAX* genes; this was particularly noticeable for the repression of *AUX1* and *LAX1* genes (Fig. S2B). Unexpectedly, *AUX1* was also downregulated in *lax2-2* mutant plants and this result cannot be easily explained; it is possible that a back negative feedback or cross regulation with another gene may be occurring. The phenotypic characterization of these transgenic plants brought interesting but unexpected results. *LAX2* expression under the CaMV *35S* promoter significantly increased the inflorescence stem size (Fig. S3A). This increment in stem area resulted in the expansion of xylem size, including xylem length and number of xylem cell rows (Fig. 6A, B; Fig. S3B). However, the proportion of xylem to total stem area (xylem area/total stem area) was restored to WT levels in the *lax2-2* plants overexpressing *LAX2* (Fig. 6C). Moreover, *LAX2* ectopic expression in the *lax2-2* genetic background also restored the leaf venation symmetry to WT levels (Fig. 7A), displaying a similar distance between the attachment sites of the third vein pair (Fig. 7B), and a similar lateral-vein asymmetry index (Fig. 7C) to WT leaves. These results suggested that LAX2 is able to modulate xylem development.

Expression of HaHB4 *in transgenic soybean increases vascular asymmetry in leaves*

HaHB4 expression driven by its native promoter in transgenic soybean plants improves yield and drought tolerance in the field (Chan and Gonzalez, 2015). This biotechnological event, originally called *b10H*, was used to test the hypothesis of whether *HaHB4* is able to induce changes in soybean leaves similar to those observed in transgenic Arabidopsis plants, i.e. changes in xylem ratio and vascular innervations in leaves. To test this hypothesis, we scored the vein asymmetry ratio in the terminal foliole of the last fully developed leaf of V7 soybean plants (*Glycine max* 'Williams 82') grown in the glasshouse. We quantified the xylem ratio in basal epicotyl cross-sections and found no difference between transformed and WT individuals (Supplementary Data Fig. S4A-C). On the other hand, we observed that vein attachment sites were more asymmetrically distributed in the *b10H* soybean leaves than in the WT (Fig. 8A). Indeed, the vein asymmetry ratio was significantly higher in the former than in the latter (Fig. 8B). Then, we wondered if water deficit might also influence this phenotypic trait. As expected, stomatal conductance was reduced among water-stressed plants (Fig. S5A). We did not find significant differences in stomatal conductance between WT and *b10H* genotypes grown under

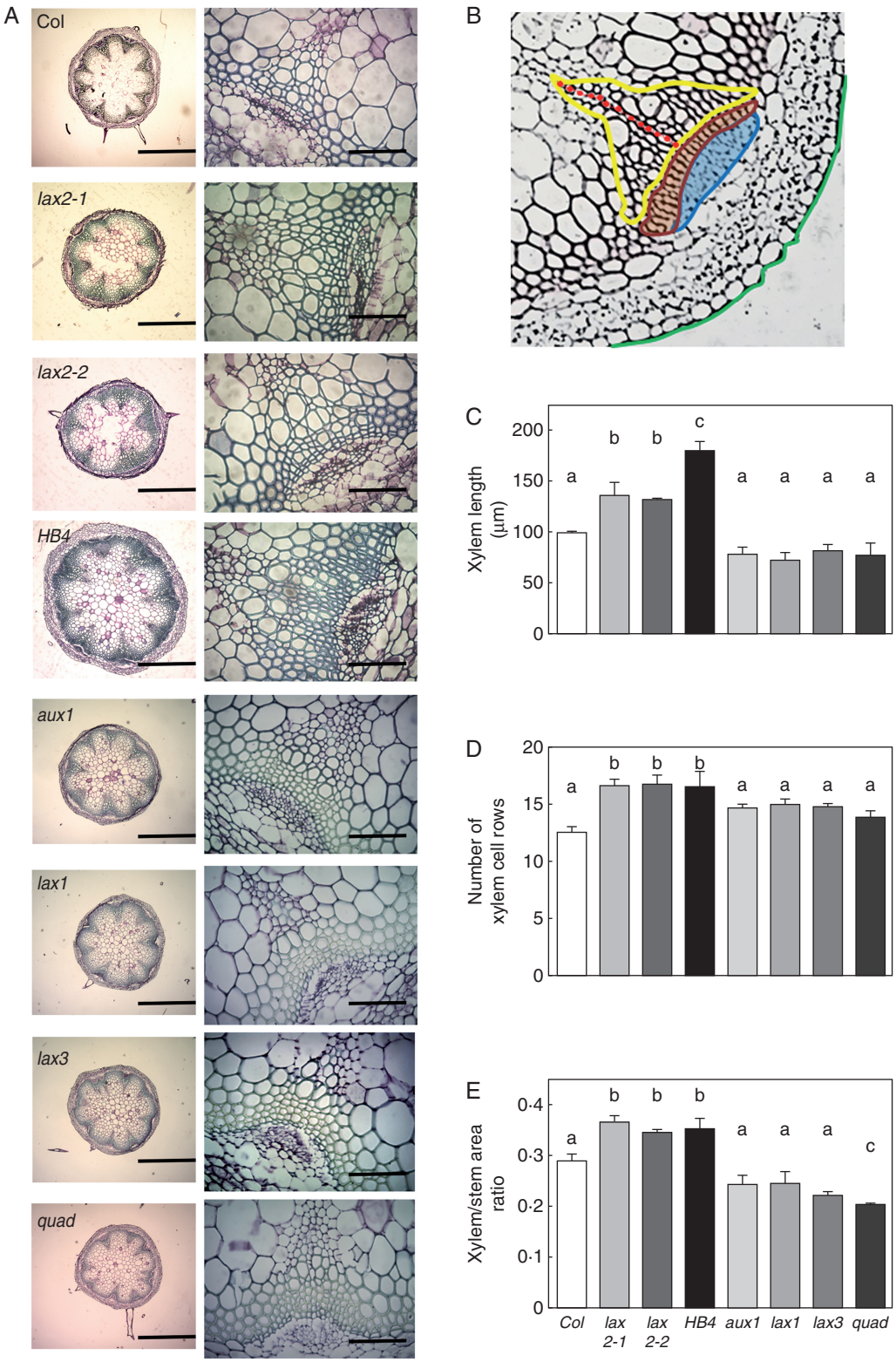

FIG. 4. Both *lax2* mutants and *35:HaHB4* plants show an enhanced proportion of xylem in the main inflorescence stem. (A) Illustrative photographs of basal shoot cross-section of inflorescence stems together with a picture inset showing a zoom on a representative vascular bundle for analysed genotypes. Basal shoot scale bar represents 0·5 mm, whereas vascular-bundle inset scale bar represents 0·1 mm. (B) Illustration of a vascular bundle showing measured parameters as follows: yellow line is the total xylem area; red dots are xylem cell row along the main xylem axis; green dashed line illustrates a portion of the total stem area considered for xylem/stem area ratio. Procambial cells are enclosed in orange. The blue area indicates phloem cells. Column bar graphs of: (C) xylem length, (D) number of xylem cell rows and (E) xylem/stem area ratio. Vascular bundle parameters were taken from pictures of basal shoot cross-section of inflorescence stems for different genotypes, including Col-0, *lax2-1*, *lax2-2*, *35S:HaHB4*, *aux1-21*, *lax1*, *lax3* and *quad*. Thin bars represent s.e. Different letters indicate significant differences ($P < 0{\cdot}05$, Tukey test).

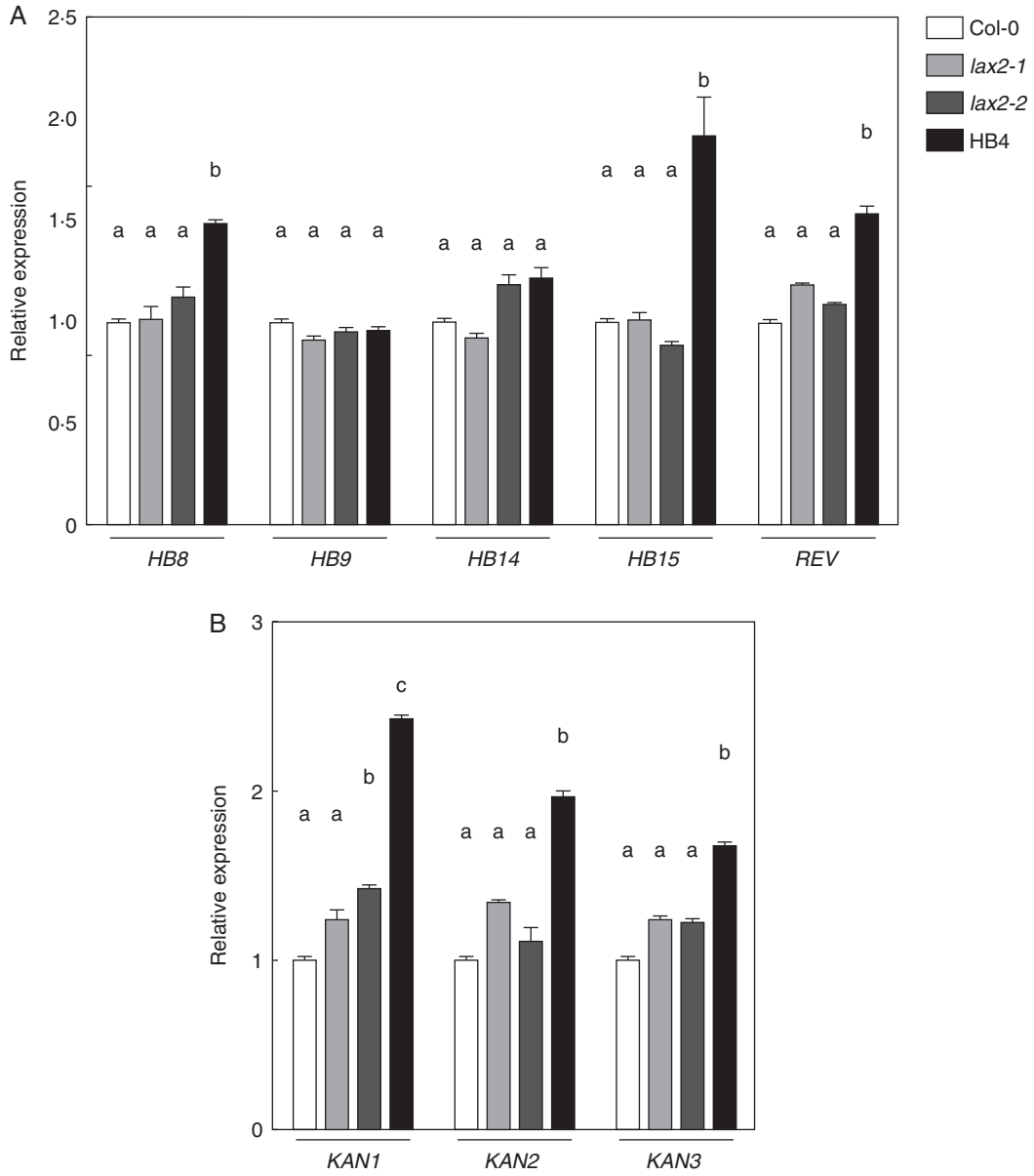

FIG. 5. Expression levels of Arabidopsis transcription factors involved in vascular development. Relative transcript levels of *HD-ZIP III* (A) and *KANADI* (B) genes were quantified by RT-qPCR using RNAs isolated from the last 3 cm of inflorescence stem excluding flower buds. Different letters indicate significant differences ($P < 0{\cdot}05$, Tukey test).

water deficit (Fig. S5A). Further experiments under field conditions will be relevant to shed light on this subject. We observed that the vein asymmetry ratio did not change significantly upon water deprivation (Fig. S5B). In other words, the vein asymmetry ratio was somehow independent of the plant water status. This result confirmed that soybean plants bearing the *HaHB4* gene behave similar to *35S:HaHB4* Arabidopsis plants, inducing an increased asymmetry on leaf venation.

HaHB4 *down-regulates the expression of* GmLAX *genes in transgenic soybean*

We wondered if this increased asymmetry in the venation patterning of *b10H* soybean leaves could be related, as well as in Arabidopsis, to the repression of *LAX* genes. We developed a BLAT (BLAST-like Alignment Tool) search on the soybean genome for exact or nearly exact coincidences representative of robust hits. This search allowed us to identify nine putative *GmLAX* genes with high protein sequence similarity (> 95%) to the AtLAX2 protein sequence. We then selected at least one best BLAT soybean hit for each member of the Arabidopsis *AUX/LAX* family and performed RT-qPCR measurements. In total, we tested the transcript levels of six out of nine putative *GmLAX* genes in the same foliole used to estimate venation patterning. Based on the RT-qPCR quantifications we showed that the expression of four out of six *GmLAX* genes was significantly repressed in *b10H* leaves as compared to the control genotype (Fig. 8C).

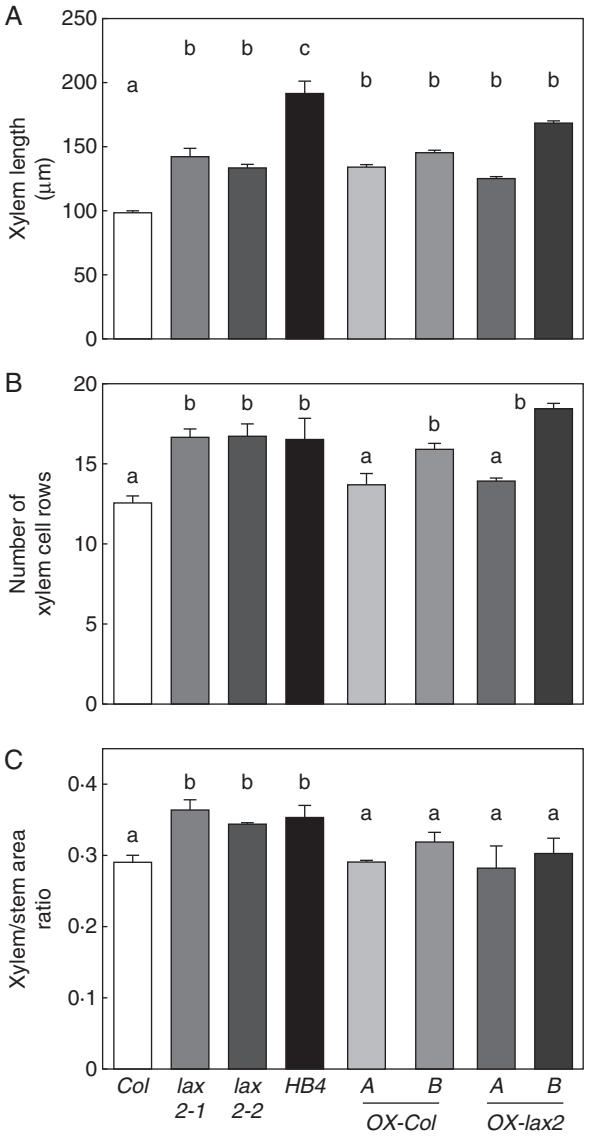

FIG. 6. Ectopic expression of *LAX2* in Arabidopsis transgenic plants restores the xylem/stem area ratio of *lax2* mutants. Column bar graphs represent (A) the xylem length, (B) the number of xylem cell rows and (C) the xylem/total stem area ratio in basal shoot cross-sections of stems. Basal shoot cross-sections of transgenic *35S:mCitrine:LAX2* stems were used to measure vascular bundle parameters. Thin bars represent s.e. Different letters indicate significant differences ($P < 0{\cdot}05$, Tukey test).

DISCUSSION

Here, we report that the ectopic expression of *HaHB4* in Arabidopsis and soybean plants repressed the expression of *LAX2*, or *AUX/LAX* homologue genes from soybean, and induced changes in leaf venation patterning in both heterologous species. Such changes were also observed in *lax2* mutant plants, suggesting a key role of *LAX2* in this developmental event. It was previously reported that auxin distribution in the leaf lamina is one of the major factors controlling venation symmetry (Aloni, 2001; Aloni *et al*., 2003). In the context of vascular development, it was also shown that the *lax2* mutant exhibited vascular breaks in cotyledons (Peret *et al*., 2012). More recently, a computational approach suggested that AUX/LAX influx carriers were required for vascular patterning (Fabregas *et al*., 2015). In this regard, it was experimentally shown that the *quad* mutant developed fewer and less-dense vascular bundles than the WT, not balanced with the formation of xylem cells (number and size) both in shoots and roots (Fabregas *et al*., 2015). This evidence supported a role for auxin influx carriers on xylem development, and together with the fact that microarray data and RT-qPCR matched *HaHB4* in the ability to downregulate the expression of *LAX2* in Arabidopsis plants, led us to explore the venation patterning and xylem development on *lax2* mutants. In agreement with our hypothesis, *lax2-1* and *lax2-2* mutant leaves had an altered symmetry in the distribution of lateral-vein attachment sites and consequently in their lateral-vein asymmetry index, similar to those observed in *35S:HaHB4* plants (Fig. 2B–D). The differential phenotypes of the *lax2* mutant were complemented with a WT copy of the *LAX2* gene, indicating that auxin homeostasis in plant tissues is critical to achieve a normal leaf venation symmetry and normal xylem development (Fig. 7). It is important to mention that a previous report using an N-terminal translational fusion between AUX1 protein and the yellow fluorescent protein (N-YFP-AUX1) failed to restore the root gravitropic response of the null *aux1-22* mutant (Swarup *et al*., 2004). In this paper, we used a different vector to create an N-terminal fusion protein between mCitrine and LAX2. This protein chimera was able to restore venation patterning and xylem development of the *lax2-2* mutant. The different behaviour of comparable constructs might arise from intrinsic differences of the translational fusion proteins or from expression levels derived from different vector backbones. The overexpression of *LAX2* complemented the mutant phenotype but did not generate a differential opposite phenotype, in either the mutant or the WT background plants. This observation can be explained by *LAX2* expression reaching a certain threshold level and other mechanisms controlling the activity and/or amount of auxin transporters. In this context, it might be relevant to explore the ability of HaHB4 to restore the *lax2* mutant phenotype. However, we can suggest that a complementation with HaHB4, or with an Arabidopsis HD-Zip I gene, would not be able to restore the differential *lax2-2* phenotype because our evidence suggests that it would be acting upstream of LAX2. However, this question is still open and further experiments are in course to obtain a better understanding of this scenario.

Our results suggest that LAX2 protein levels are required to modulate *AUX1* gene expression. As was previously suggested by other research groups, there is a complex regulation of the different auxin transporters and such regulation might be dependent on the cell niche of expression. Kasprzewska *et al*. (2015) described experiments performed using *ProLAX1:GUS* and *ProLAX2:GUS* fusion constructs in which both *LAX1* or *LAX2* promoter activities were similar in young true leaves of the *quad* mutant and wild-type plants. However, at the root cellular level, LAX2 and LAX3 were somehow absent in AUX1-expressing cells, either when *LAX2* or when *LAX3* were expressed under the control of the *AUX1* promoter or fused to YFP under the control of a CAMV 35S promoter (Peret *et al*., 2012). Taken together, these results support the fact that *AUX/LAX* gene expression patterns and protein levels in the cell might be regulated by the abundance of other AUX/LAX members.

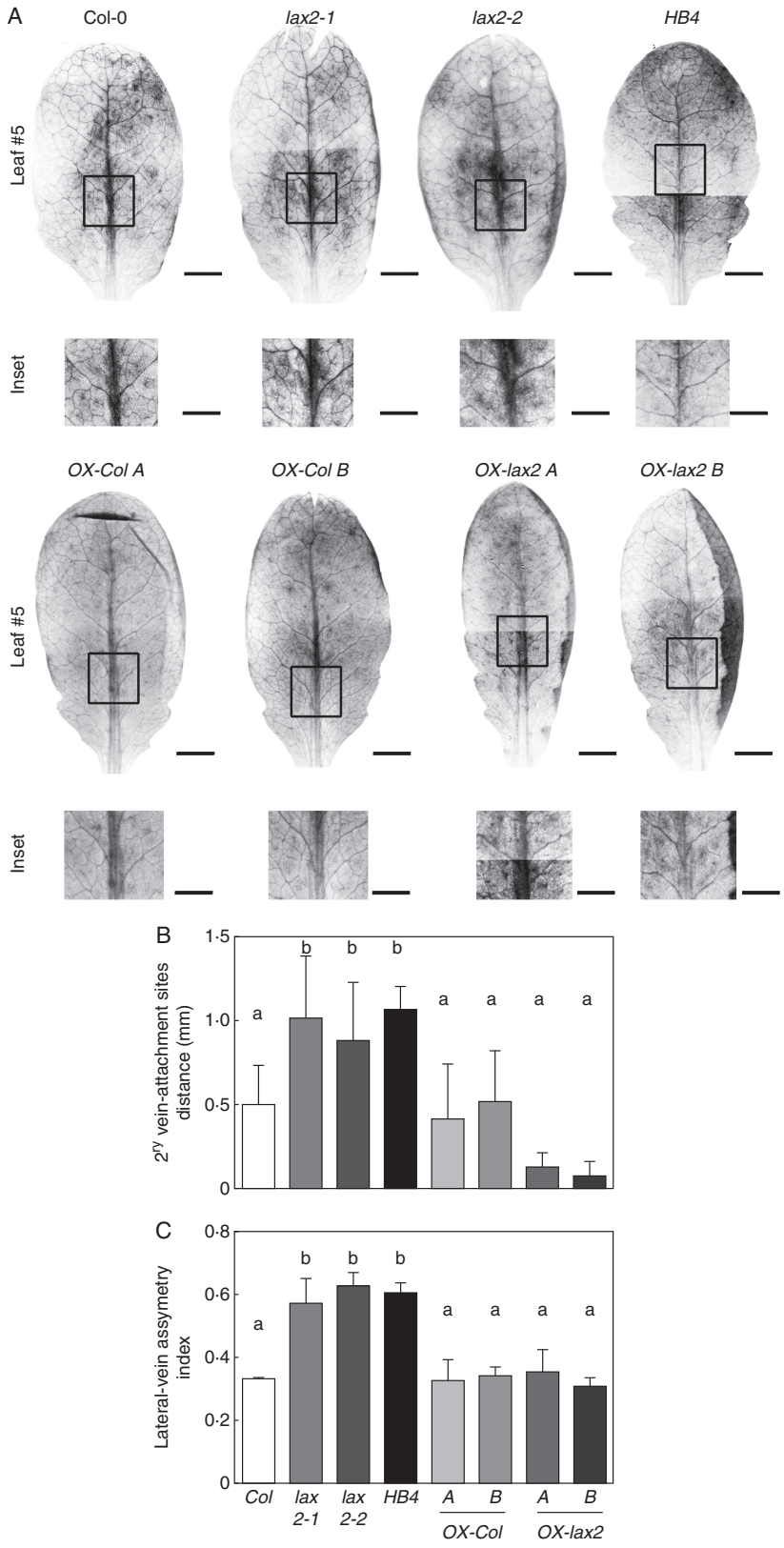

FIG. 7. Ectopic expression of *LAX2* in Arabidopsis transgenic plants restores venation patterning in leaves of *lax2* mutants. (A) Illustrative photographs of leaf number 5 and the corresponding inset showing a zoom on the third vein pair. The final image resulted from merging two photographs. Whole-leaf scale bar represents 2·0 mm, whereas leaf-inset scale bar represents 1·0 mm. (B) Average distance between the two attachment sites of the lateral veins of the third vascular pair. (C) Lateral-vein asymmetry index. Thin bars represent s.e.. Different letters indicate significant differences ($P < 0{\cdot}05$, Tukey test).

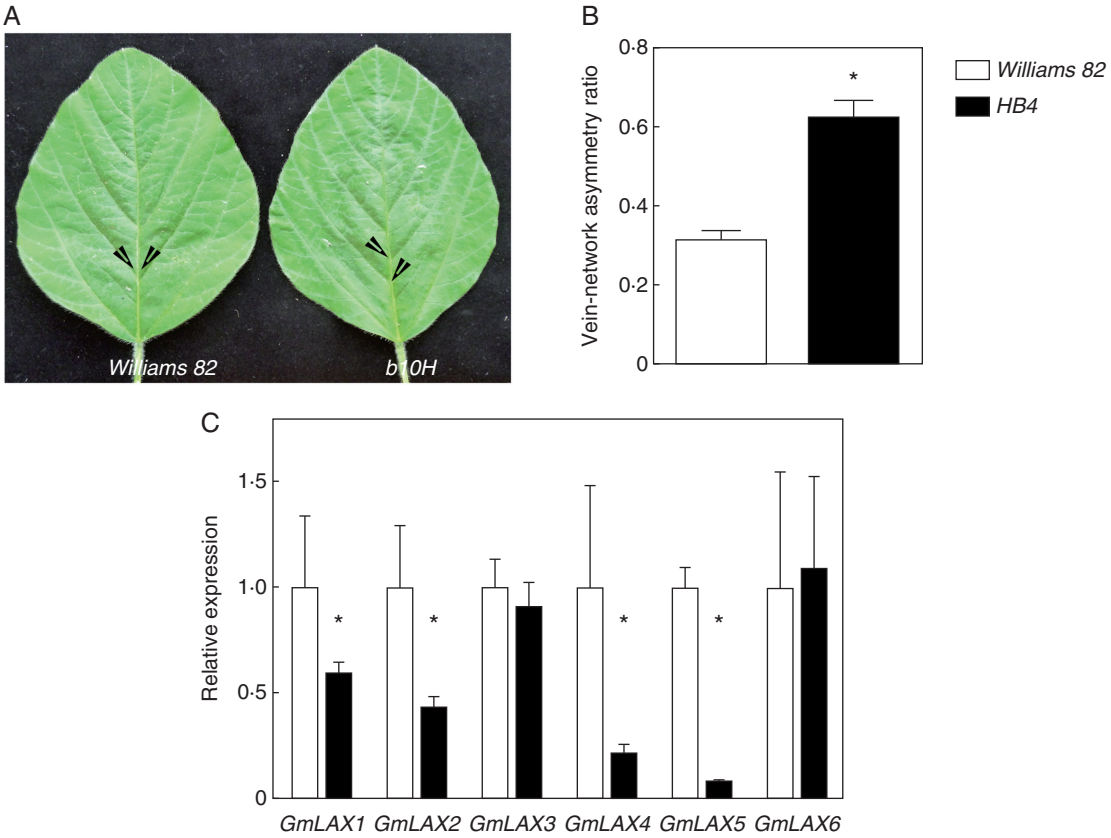

FIG. 8. Ectopic expression of *HaHB4* in transgenic soybean leaves enhances the asymmetric formation of secondary vein pairs. (A) Illustrative photographs of the terminal foliole. White arrowheads indicate development start sites of different vein pairs. Scale bar represents 3 cm. (B) Fraction of asymmetric attachment sites compared to the total lateral vein pairs in the foliole. A total of three replicates were used to calculate the s.e. Differences were considered significant at $*P < 0{\cdot}05$ (Student's *t*-test). (C) *GmLAX* transcript levels detected by RT-qPCR using total RNA isolated from soybean third foliole of a fully expanded leaf. Measurements were taken on the terminal foliole from the last fully developed leaf corresponding to a 30-d-old soybean plant (V7 stage). Error bars represent the s.e. of three independent biological replicates. Statistical significance was computed by Student's *t*-test. $*P < 0.05$.

HD-Zip III and KANADI TFs are well-known regulators of xylem and phloem development. The resulting organization of the vascular bundle relies on a fine interplay between these two kinds of TFs (Ilegems *et al*., 2010; Schuetz *et al*., 2013). HD-Zip III TFs are positive regulators of polar auxin transport triggering xylem development, and their expression is auxin dependent (Ilegems *et al*., 2010; Huang *et al*., 2014; Ursache *et al*., 2014; De Rybel *et al*., 2016; Müller *et al*., 2016). In parallel, mobile peptides are synthesized in phloem cells to inhibit xylem differentiation from procambium cells. The ectopic expression of *HaHB4*, and the mutation of *LAX2* increased the xylem/stem area ratio (xylem area/total stem area) in the inflorescence stem of Arabidopsis plants. Despite the fact that we did not detect differential expression of HD-Zip III and KANADI TFs on the terminal inflorescence stem of *lax2* mutants, we cannot rule out the possibility that AUX/LAX proteins might control their expression at specific cell niches. It is noteworthy that it has been recently shown that KAN and REV regulate the expression of *LAX1*, *LAX2* and *LAX3* genes (Baima *et al*., 2014; Huang *et al*., 2014). Further experiments are needed to test this hypothesis. In contrast, ectopic expression of *HaHB4* clearly altered the expression pattern of several HD-Zip III and KANADI TFs at the inflorescence stem, which might be part of the observed changes in vascular architecture of the transgenic plants.

Although it is known that HaHB4 generates a complex phenotype, including insensitivity to ethylene and induction of jasmonic acid biosynthesis (Manavella *et al*., 2006, 2008), we can strongly suggest that the effect of this sunflower TF on leaf venation and xylem architecture is, at least in part, orchestrated by *LAX2*. It is tempting to speculate that *HaHB4*-induced modulation of *LAX2* expression, and therefore of auxin accumulation patterns in the leaf, might be responsible for the enhanced asymmetry of leaf venation patterning. This model is supported by a rise in the lateral-vein asymmetry index in transgenic soybean leaves, where the ectopic expression of *HaHB4* was also accompanied by a broad downregulation of several *GmLAX* genes.

Previously, HD-Zip I proteins had been largely linked to plant acclimation responses to biotic and abiotic environmental factors as well as influencing the plant's ability to perceive and trigger hormonal signals, i.e. ethylene and abscisic acid (Manavella *et al*., 2006; Lechner *et al*., 2011; Perotti *et al*., 2017). More recently, some HD-Zip I members were involved in different developmental processes unrelated to stress or hormones. For example, ATHB16 was shown to be a positive regulator of growth responses (Wang *et al*., 2003), whereas ATHB12 turned

out to act as a negative regulator of the same response (Hur *et al*., 2015) and the paralogous pair AtHB13/23 were described as negative regulators of inflorescence stem elongation (Ribone *et al*., 2015). Our study shows that the ectopic expression of *HaHB4* in heterologous plant species modulates venation patterning in leaves and xylem development in the inflorescence stem. In this context, it will be relevant to explore if the *HaHB4* mechanism is based on the ability to directly modulate *LAX2* expression, or if it is part of a broader impact on auxin accumulation that ends up on the regulation of HD-Zip III TFs. As already noted, it was recently shown that both KAN and REV are able to modulate *LAX* gene expression (Baima *et al*., 2014; Huang *et al*., 2014). Further experiments are needed to explore the role of Arabidopsis HD-Zip I TFs on venation patterning and xylem architecture using HD-Zip I Arabidopsis mutants and overexpressing lines. This work opens a novel perspective for the study of vascular pattering in crops and its potential impact in the physiology of economically relevant plants.

SUPPLEMENTARY DATA

Supplementary data are available online at https://academic.oup.com/aob and consist of the following. Fig. S1: additional architecture traits were similar between *lax2* mutants and *35S:HaHB4* plants as compared to control plants. Fig. S2: *LAX2* expression levels in Col-0 and *lax2* mutant plants transformed with *35S:mCitrine:LAX2*. Fig. S3: Ectopic expression of *LAX2* in Arabidopsis transgenic plants restores the xylem/stem area ratio of *lax2* mutants. Fig. S4: Xylem/stem area ratio in transgenic soybean stems bearing the *HaHB4* gene controlled by its native promoter. Fig. S5: water-deficit stress treatment does not induce significant changes in leaf venation symmetry. Table S1: list of primers used in this study for RT-qPCR. Table S2: list of 446 genes clustered according to the co-expression analysis performed with AtGenExpress public microarray data. Each gene was assigned to a cluster which was identified with a number. Some clusters include only one gene. Affymetrix probeset identifier, TAIR identifier and gene symbols are provided.

ACKNOWLEDGEMENTS

This work was supported by Agencia Nacional de Promoción Científica y Tecnológica (PICT 2014 3300 to RLC and PICT 2013-0099 to JEM), and Universidad Nacional del Litoral (UNL). JEM, JVC, MEO and RLC are CONICET career members. GSMP and ALA were post-doctoral fellows of CONICET. We thank Dr Ranjan Swarup for kindly providing *aux*/*lax* single and quadruple mutant seeds used in this study and Dr Detlef Weigel for the pJV126 vector. GSMP, JEM and RLC conceived and designed the experiments. GSMP, JEM, JVC and MEO performed the experiments. GSMP, JEM, ALA and RLC analysed the data. ALA performed the computational analysis. JEM and RLC wrote the paper.

LITERATURE CITED

Aloni R. 2001. Foliar and axial aspects of vascular differentiation: hypotheses and evidence. *Journal of Plant Growth Regulation* **20**: 22–34.

Aloni R. 2010. The induction of vascular tissues by auxin. In: Davies PJ, ed. *Plant hormones: biosynthesis, signal transduction, action!* Dordrecht: Springer Netherlands, 485–518.

Aloni R, Schwalm K, Langhans M, Ullrich CI. 2003. Gradual shifts in sites of free-auxin production during leaf-primordium development and their role in vascular differentiation and leaf morphogenesis in Arabidopsis. *Planta* **216**: 841–853.

Arcadia-Biosciences. 2015. Verdeca's HB4 stress tolerance trait completes US Food and Drug Administration early food safety evaluation. http://www.arcadiabio.com/news/press-release/verdeca%E2%80%99s-hb4-stress-tolerance-trait-completes-us-food-and-drug-administration.

Arce AL, Raineri J, Capella M, Cabello JV, Chan RL. 2011. Uncharacterized conserved motifs outside the HD-Zip domain in HD-Zip subfamily I transcription factors; a potential source of functional diversity. *BMC Plant Biology* **11**: 42.

Baima S, Forte V, Possenti M, *et al.* 2014. Negative feedback regulation of auxin signaling by ATHB8/ACL5-BUD2 transcription module. *Molecular Plant* **7**: 1006–1025.

Bainbridge K, Guyomarc'h S, Bayer E, *et al.* 2008. Auxin influx carriers stabilize phyllotactic patterning. *Genes and Development* **22**: 810–823.

Boyes DC, Zayed AM, Ascenzi R, *et al.* 2001. Growth stage-based phenotypic analysis of Arabidopsis: a model for high throughput functional genomics in plants. *The Plant Cell* **13**, 1499–1510.

Capella M, Ribone PA, Arce AL, Chan RL. 2015*a*. *Arabidopsis thaliana* HomeoBox 1 (AtHB1), a Homedomain-Leucine Zipper I (HD-Zip I) transcription factor, is regulated by PHYTOCHROME-INTERACTING FACTOR 1 to promote hypocotyl elongation. *New Phytologist* **207**: 669–682.

Capella M, Ribone PA, Arce AL, Chan RL. 2015*b*. Homeodomain–leucine zipper transcription factors: structural features of these proteins, unique to plants. In: Gonzalez DH, ed. *Plant transcription factors*. Boston: Academic Press, 113–126.

Chan RL, Gonzalez DH. 2015. Modified *Helianthus annuus* transcription factor improves yield. USA. US 2013/0263327.

Chitwood DH, Headland LR, Ranjan A, *et al.* 2012. Leaf asymmetry as a developmental constraint imposed by auxin-dependent phyllotactic patterning. *The Plant Cell* **24**: 2318–2327.

Clough SJ, Bent AF. 1998. Floral dip: a simplified method for Agrobacterium-mediated transformation of *Arabidopsis thaliana*. *The Plant Journal* **16**: 735–743.

De Rybel B, Mahonen AP, Helariutta Y, Weijers D. 2016. Plant vascular development: from early specification to differentiation. *Nature Reviews Molecular Cell Biology* **17**: 30–40.

Dezar CA, Gago GM, González DH, Chan RL. 2005. Hahb-4, a sunflower homeobox-leucine zipper gene, is a developmental regulator and confers drought tolerance to *Arabidopsis thaliana* plants. *Transgenic Research* **14**: 429–440.

Fabregas N, Formosa-Jordan P, Confraria A, *et al.* 2015. Auxin influx carriers control vascular patterning and xylem differentiation in *Arabidopsis thaliana*. *PLoS Genetics* **11**, e1005183.

Farmer E, Mousavi S, Lenglet A. 2013. Leaf numbering for experiments on long distance signalling in Arabidopsis. *Protocol Exchange* doi:10.1038/protex.2013.071.

Graham J, Whitesell M, Ii M, Hel-Or H, Nevo E, Raz S. 2015. Fluctuating asymmetry of plant leaves: batch processing with LAMINA and continuous symmetry measures. *Symmetry* **7**: 255–268.

Hellens RP, Edwards EA, Leyland NR, Bean S, Mullineaux PM. 2000. pGreen: a versatile and flexible binary Ti vector for *Agrobacterium*-mediated plant transformation. *Plant Molecular Biology* **42**: 819–832.

Houchmandzadeh B, Wieschaus E, Leibler S. 2002. Establishment of developmental precision and proportions in the early *Drosophila* embryo. *Nature* **415**: 798–802.

Huang T, Harrar Y, Lin C, *et al.* 2014. Arabidopsis KANADI1 acts as a transcriptional repressor by interacting with a specific cis-element and regulates auxin biosynthesis, transport, and signaling in opposition to HD-ZIPIII factors. *The Plant Cell* **26**: 246–262.

Hur YS, Um JH, Kim S, *et al.* 2015. *Arabidopsis thaliana* homeobox 12 (ATHB12), a homeodomain-leucine zipper protein, regulates leaf growth by promoting cell expansion and endoreduplication. *New Phytologist* **205**: 316–328.

Ilegems M, Douet V, Meylan-Bettex M, *et al.* 2010. Interplay of auxin, KANADI and Class III HD-ZIP transcription factors in vascular tissue formation. *Development* **137**: 975–984.

Kasprzewska A, Carter R, Swarup R, *et al.* 2015. Auxin influx importers modulate serration along the leaf margin. *The Plant Journal* **83**: 705–718.

Kilian J, Whitehead D, Horak J, *et al.* 2007. The AtGenExpress global stress expression data set: protocols, evaluation and model data analysis of UV-B light, drought and cold stress responses. *The Plant Journal* **50**: 347–363.

Klingenberg CP, McIntyre GS, Zaklan SD. 1998. Left-right asymmetry of fly wings and the evolution of body axes. *Proceedings of the Royal Society Biological Sciences* **265**: 1255–1259.

Koizumi K, Sugiyama M, Fukuda H. 2000. A series of novel mutants of *Arabidopsis thaliana* that are defective in the formation of continuous vascular network: calling the auxin signal flow canalization hypothesis into question. *Development* **127**: 3197–3204.

Leamy LJ, Klingenberg CP. 2005. The genetics and evolution of fluctuating asymmetry. *Annual Review of Ecology, Evolution, and Systematics* **36**: 1–21.

Leamy LJ, Routman EJ, Cheverud JM. 2002. An epistatic genetic basis for fluctuating asymmetry of mandible size in mice. *Evolution* **56**: 642–653.

Lechner E, Leonhardt N, Eisler H, *et al.* 2011. MATH/BTB CRL3 receptors target the homeodomain-leucine zipper ATHB6 to modulate abscisic acid signaling. *Developmental Cell* **21**: 1116–1128.

Lempe J, Lachowiec J, Sullivan AM, Queitsch C. 2013. Molecular mechanisms of robustness in plants. *Current Opinion in Plant Biology* **16**: 62–69.

Lucas WJ, Groover A, Lichtenberger R, *et al.* 2013. The plant vascular system: evolution, development and functions. *Journal of Integrative Plant Biology* **55**: 294–388.

Manavella PA, Arce AL, Dezar CA, *et al.* 2006. Cross-talk between ethylene and drought signalling pathways is mediated by the sunflower Hahb-4 transcription factor. *The Plant Journal* **48**: 125–137.

Manavella PA, Dezar CA, Bonaventure G, Baldwin IT, Chan RL. 2008. HAHB4, a sunflower HD-Zip protein, integrates signals from the jasmonic acid and ethylene pathways during wounding and biotic stress responses. *The Plant Journal* **56**: 376–388.

Masel J, Siegal ML. 2009. Robustness: mechanisms and consequences. *Trends in Genetics* **25**: 395–403.

Mattsson J, Sung ZR, Berleth T. 1999. Responses of plant vascular systems to auxin transport inhibition. *Development* **126**: 2979–2991.

Müller CJ, Valdés AE, Wang G, *et al.* 2016. PHABULOSA mediates an auxin signaling loop to regulate vascular patterning in Arabidopsis. *Plant Physiology* **170**: 956–970.

Muñoz-Nortes T, Wilson-Sánchez D, Candela H, Micol JL. 2014. Symmetry, asymmetry, and the cell cycle in plants: known knowns and some known unknowns. *Journal of Experimental Botany* **65**: 2645–2655.

Payne JL, Wagner A. 2015. Mechanisms of mutational robustness in transcriptional regulation. *Frontiers in Genetics* **6**: 322.

Peret B, Swarup K, Ferguson A, *et al.* 2012. AUX/LAX genes encode a family of auxin influx transporters that perform distinct functions during Arabidopsis development. *The Plant Cell* **24**: 2874–2885.

Perotti MF, Ribone PA, Chan RL. 2017. Plant transcription factors from the Homeodomain-Leucine Zipper family I. Role in development and stress responses. *IUBMB Life* **69**: 280–289.

Petrasek J, Friml J. 2009. Auxin transport routes in plant development. *Development* **136**: 2675–2688.

Prado K, Maurel C. 2013. Regulation of leaf hydraulics: from molecular to whole plant levels. *Frontiers in Plant Science* **4**: 255.

Queitsch C, Sangster TA, Lindquist S. 2002. Hsp90 as a capacitor of phenotypic variation. *Nature* **417**: 618–624.

Ribone PA, Capella M, Chan RL. 2015. Functional characterization of the homeodomain leucine zipper I transcription factor AtHB13 reveals a crucial role in Arabidopsis development. *Journal of Experimental Botany* **66**: 5929–5943.

Rutherford SL, Lindquist S. 1998. Hsp90 as a capacitor for morphological evolution. *Nature* **396**: 336–342.

Salehin M, Bagchi R, Estelle M. 2015. SCFTIR1/AFB-based auxin perception: mechanism and role in plant growth and development. *The Plant Cell* **27**: 9–19.

Schmid M, Davison TS, Henz SR, *et al.* 2005. A gene expression map of *Arabidopsis thaliana* development. *Nature Genetics* **37**: 501–506.

Schneider CA, Rasband WS, Eliceiri KW. 2012. NIH Image to ImageJ: 25 years of image analysis. *Nature Methods* **9**: 671–675.

Schuetz M, Smith R, Ellis B. 2013. Xylem tissue specification, patterning, and differentiation mechanisms. *Journal of Experimental Botany* **64**: 11–31.

Sieburth LE. 1999. Auxin is required for leaf vein pattern in Arabidopsis. *Plant Physiology* **121**: 1179–1190.

Swarup K, Benkova E, Swarup R, *et al.* 2008. The auxin influx carrier LAX3 promotes lateral root emergence. *Nature Cell Biology* **10**: 946–954.

Swarup R, Kargul J, Marchant A, *et al.* 2004. Structure-function analysis of the presumptive Arabidopsis auxin permease AUX1. *The Plant Cell* **16**: 3069–3083.

Swarup R, Kramer EM, Perry P, *et al.* 2005. Root gravitropism requires lateral root cap and epidermal cells for transport and response to a mobile auxin signal. *Nature Cell Biology* **7**: 1057–1065.

Swarup R, Perry P, Hagenbeek D, *et al.* 2007. Ethylene upregulates auxin biosynthesis in Arabidopsis seedlings to enhance inhibition of root cell elongation. *The Plant Cell* **19**: 2186–2196.

Ursache R, Miyashima S, Chen Q, *et al.* 2014. Tryptophan-dependent auxin biosynthesis is required for HD-ZIP III-mediated xylem patterning. *Development* **141**: 1250–1259.

Vanneste S, Friml J. 2009. Auxin: a trigger for change in plant development. *Cell* **136**: 1005–1016.

Wang Y, Henriksson E, Soderman E, Henriksson KN, Sundberg E, Engstrom P. 2003. The Arabidopsis homeobox gene, ATHB16, regulates leaf development and the sensitivity to photoperiod in Arabidopsis. *Developmental Biology* **264**: 228–239.

Warde-Farley D, Donaldson SL, Comes O, *et al.* 2010. The GeneMANIA prediction server: biological network integration for gene prioritization and predicting gene function. *Nucleic Acids Research* **38 (Web Server issue)**: W214–220.